I. Doležel[1], P. Dvořák[2], P. Karban[2], B. Ulrych[2]
[1]Faculty of Electrical Engineering, Czech Technical University, Prague, Czech Republic
[2]Faculty of Electrical Engineering, University of West Bohemia, Pilsen, Czech Republic

DETERMINATION OF CIRCUIT PARAMETERS OF HIGH-FREQUENCY PROFILE CONDUCTORS

The paper deals with numerical computation of effective resistance and inductance of profile conductors carrying harmonic currents for a wide range of frequencies. Investigated is particularly the influence of varying profiles of the conductors for the same area of their cross-sections. The theoretical analysis is illustrated on several examples whose results are discussed.

Introduction

The resistance and inductance of profile conductors belong to their most important parameters that substantially affect their transmission abilities. Both these quantities are functions of frequency. Generally, with higher frequency their resistance grows while the inductance decreases. For frequencies to approximately hundreds kHz the distribution of the current density is the less uniform the more complicated is the circumference of the conductor (its highest values can be found at various corners while values near smooth parts are usually much lower). For even higher frequencies (starting from MHz) the depth of penetration becomes very small so that the influence of the shape of the cross-section is practically negligible. The current is now transferred practically along its perimeter and its density depends almost only on its length.

This knowledge is of fundamental importance for design of conductors for high frequency currents. Required is here the minimal possible growth of resistance at the lowest consumption of material. At the first sight, of course, it is very thin band conductors that well satisfy these requirements. But mechanical properties of such conductors are rather poor and, moreover, they would take a lot of place in *hf* devices. It is, therefore, necessary to do a compromise consisting in selection of such a profile of the conductor that secures better mechanical properties at the expense of acceptable deterioration of the mentioned circuit parameters and increase of the production costs (technology of production of these conductors is relatively complicated and based on cold drawing through diamond dies in which precise apertures of corresponding profiles are performed by ultrasound).

The paper deals with computation of the frequency-dependent resistance and inductance of several types of profile conductors and their comparison with analogous quantities of a cylindrical conductor with the same area of its cross-section.

Formulation of the technical problem

Determined are the frequency-dependent effective resistance and inductance of the profile conductors depicted in Fig. 1 (**a** - cross-type conductor, **b** - star-type conductor and **c** - band-type conductor) for several versions differing from each other by geometrical sizes. The results are compared with analogous values for the cylindrical conductor **d**. The area of cross-sections of all conductors is the same and its value $S_c = 10^{-6}$ m^2.

Mathematical model of the problem

Let us consider a long conductor carrying harmonic current of amplitude I and frequency f. The conductor, whose material is supposed uniform, isotropic and linear (with constant magnetic permeability μ_0 and electrical conductivity γ), has an arbitrary cross-section of area S_c. Its basic arrangement is depicted in Fig. 2.

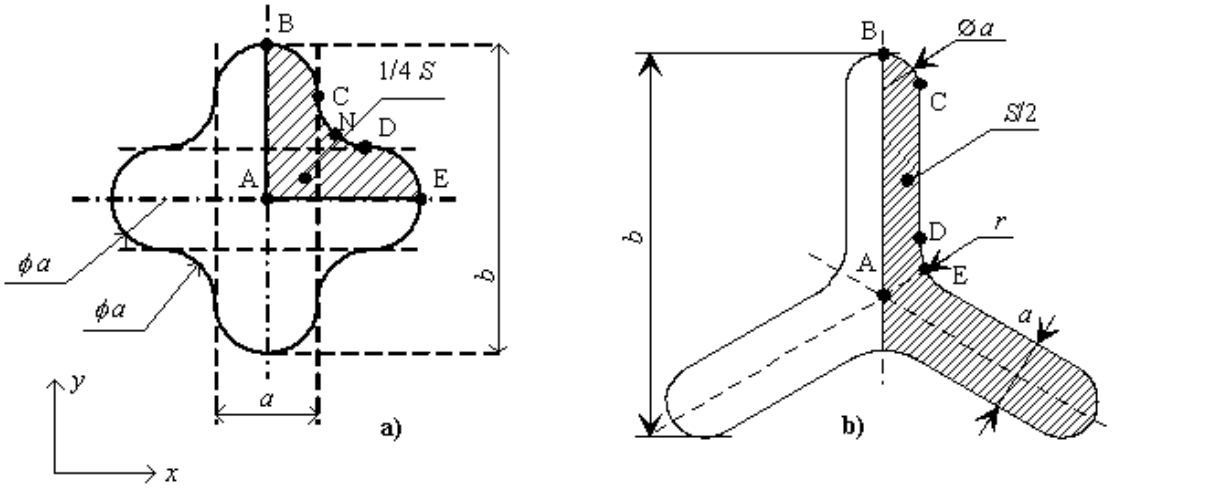

Version I: $a = 0.000437$ m, $b = 0.001372$ m
Version II: $a = 0.000384$ m, $b = 0.001536$ m
Version III: $a = 0.000337$ m, $b = 0.001686$ m

Version I: $a = 0.000360$ m, $b = 0.001594$ m, $r = 0.000623$ m
Version II: $a = 0.000329$ m, $b = 0.001706$ m, $r = 0.000570$ m

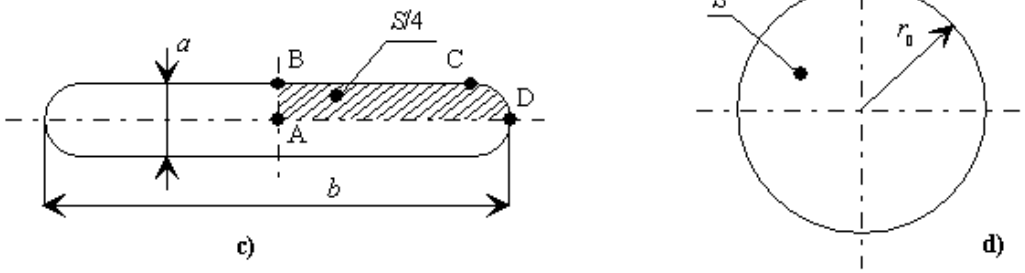

Version I: $a = 0.000160$ m, $b = 0.003196$ m
Version II: $a = 0.000130$ m, $b = 0.003900$ m
Version III: $a = 0.000112$ m, $b = 0.004496$ m

$r_0 = 0.000564$ m

Fig. 1. Considered types of conductors: ***a*** *– cross-type conductor;* ***b*** *– star-type conductor;* ***c*** *– band-type conductor;* ***d*** *– cylindrical conductor*

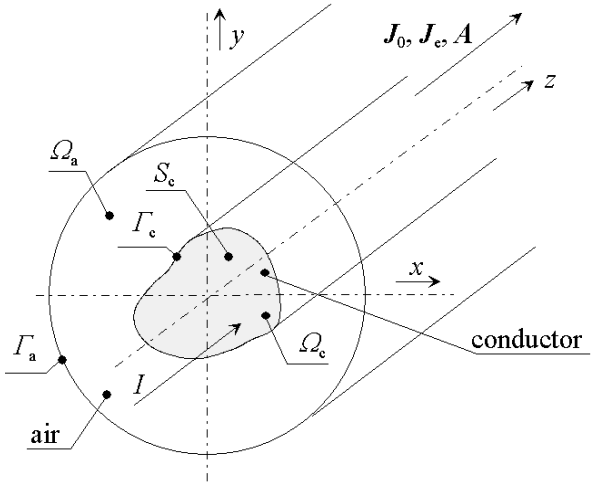

Fig. 2. General investigated arrangement

The definition area of the problem (in 2D, see Fig. 2) has to be suggested with respect to disability of determining the boundary condition along the circumference Γ_c of the conductor. That is why the area of the conductor is surrounded by sufficiently large air cylinder of cross-section Ω_a with radius R, along whose perimeter Γ_a the field distribution may be estimated with relatively good accuracy.

As all electromagnetic quantities are supposed harmonic, they may be expressed in terms of their phasors. Each of the phasors of the vector potential $\underline{\boldsymbol{A}}$ and current density $\underline{\boldsymbol{J}}$ has only one nonzero component in direction z: $\underline{A}_z(x,y)$ and $\underline{J}_z(x,y)$, respectively. The phasor of the total current density $\underline{J}_z$ in the conductor consists of two terms

$$\underline{J}_z = \underline{J}_{\mathrm{p}z} + \underline{J}_{\mathrm{e}z} \tag{1}$$

where $\underline{J}_{\mathrm{p}z}$ is the potential component given as $\underline{I}/S_{\mathrm{c}}$ and $\underline{J}_{\mathrm{e}z}$ the eddy current component. Within the conductor (area Ω_{c}) distribution of the phasor $\underline{A}_z$ of the vector potential is described by the Helmholtz equation [1]

$$\Delta \underline{A}_z - \mathrm{j}\cdot\omega\gamma\mu_0 \underline{A}_z = -\mu_0 \underline{J}_{\mathrm{p}z} \tag{2}$$

while in the air (area Ω_{a}) by the Laplace equation

$$\Delta \underline{A}_z = 0\,. \tag{3}$$

The phasor of the eddy current density $\underline{J}_{\mathrm{e}z}$ within the conductor is then expressed as

$$\underline{J}_{\mathrm{e}z} = -\mathrm{j}\cdot\omega\gamma\,\underline{A}_z\,. \tag{4}$$

The boundary conditions are expressed as follows:

- Boundary Γ_{a}: $\underline{A}_z = \mathrm{const}$.
- Boundary Γ_{c}: continuity of both $\underline{A}_z$ and its normal derivatives $\partial \underline{A}_z / \partial n$.

The unknown value of $\underline{A}_z$ along the boundary Γ_{a} follows from the indirect condition

$$\int_{\Omega_{\mathrm{c}}} \underline{J}_z \mathrm{d}S = \underline{I}\,. \tag{5}$$

The knowledge of distribution of $\underline{J}_z$ represents the starting point for finding the resistance and inductance of the conductor.

- The effective resistance R'_{eff} per unit length that may be calculated from distribution of the specific Joule losses w_{J} given as

$$w_{\mathrm{J}} = \frac{\underline{J}_z \cdot \underline{J}_z^*}{\gamma} \tag{6}$$

The total Joule losses per unit length ΔP_{J} are

$$\Delta P_{\mathrm{J}} = \int_{\Omega_{\mathrm{c}}} w_{\mathrm{J}} \cdot \mathrm{d}S \tag{7}$$

and

$$R'_{\mathrm{eff}} = \frac{\Delta P_{\mathrm{J}}}{|\underline{I}|^2} = \frac{1}{|\underline{I}|^2}\int_{\Omega_{\mathrm{c}}} w_{\mathrm{J}} \cdot \mathrm{d}S\,. \tag{8}$$

- The effective inductance L'_{eff} per unit length that can be calculated from the total magnetic field energy per unit length

$$W'_{\mathrm{m}} = \frac{1}{2\mu_0}\int_{\Omega} |\underline{\boldsymbol{B}}|^2 \mathrm{d}S,\ \ \Omega = \Omega_{\mathrm{c}} \cup \Omega_{\mathrm{a}} \tag{9}$$

which gives, after some rearrangements

$$L'_{\mathrm{eff}} = \frac{2W'_{\mathrm{m}}}{|\underline{I}|^2} = \frac{\int_{\Omega} \left| \left(\frac{\partial \underline{A}_{\mathrm{z}}}{\partial x} \right)^2 + \left(\frac{\partial \underline{A}_{\mathrm{z}}}{\partial y} \right)^2 \right| \mathrm{d}S}{\mu_0 \cdot |\underline{I}|^2}\,. \tag{10}$$

The resultant effective impedance Z'_{eff} per unit length is finally given by formula

$$\underline{Z}'_{\mathrm{eff}} = R'_{\mathrm{eff}} + \mathrm{j}\cdot\omega L'_{\mathrm{eff}}\,. \tag{11}$$

Computation of the described mathematical model was realised by combination of the FEM-based professional code QuickField 5 [2] and several single-purpose user procedures developed and written by the authors in Matlab 6.5. The results were thoroughly tested with respect to their geometrical convergence discussed later on.

Examples of computation

Investigated was dependence of the effective impedance per unit length $Z'_{\text{eff}} = R'_{\text{eff}} + \text{j}\cdot\omega L'_{\text{eff}}$ on frequency f within the range 50 Hz – 50 GHz for copper ($\gamma = 5.7\cdot 10^7$ S/m) conductors of

- type **a** (Fig. 1) in versions I, II and III,
- type **b** (Fig. 1) in versions I and II,
- type **c** (Fig. 1) in versions I, II and III.

The results are compared with the similar dependence for a reference copper conductor of circular cross-section (type **d**, Fig. 1).

Conductor of type **a**

Fig. 3 shows the complete definition area of the problem (which represents one fourth of the real arrangement).

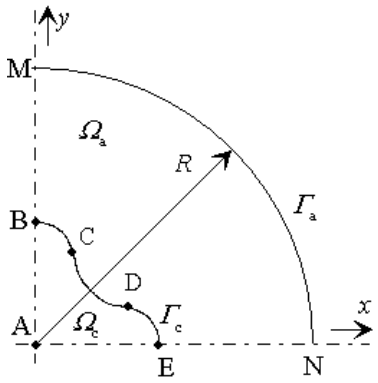

Fig. 3. Definition area of the problem

The letter R in Fig. 3 denotes radius of the artificial boundary Γ_{a} (its value being chosen in such a manner that energy of the magnetic field does not change more than by 5% when R increases by 0.01 m).

Fig. 4 shows the convergence of results as a function of the number of nodes in the mesh for frequency $f = 500$ kHz. The vertical axis shows differences of the magnetic energy in percents. It is obvious that the convergence rate depends on the shape of the profile. Let us define accuracy $W = 100\left(W_{N_2} - W_{N_1}\right)/W_{N_2}$ where W_{N_1} is total magnetic energy calculated on a grid with N_1 nodes and W_{N_2} on a grid with N_2 nodes. While in case of the circular conductor the accuracy 5% is reached for about 100000 nodes, the same accuracy for the cross-type conductor, version III (Fig.1) is reached only on a grid five times denser (about 500000 nodes). This is closely associated with distribution of magnetic field over particular cross-sections of different conductors.

Fig. 5.1 depicts the frequency-dependent ratio of the effective resistance R'_{eff} per unit length of the conductor of type **a** for all three versions and direct-current resistance R'_0 of the circular conductor of the same cross-section. Because the differences between particular curves are not too much observable, Fig. 5.2 shows their zoom for higher frequencies. It is apparent that the dependence of the effective resistance of the conductor on its profile is more substantial only at high frequencies, in this case about 10^{10} Hz and more. Only now the currents are concentrated in such a thin surface layer that the resistance depends practically only on the perimeter of the conductor.

The same dependencies have been calculated for two versions of the conductor of type **b**. Fig. 7 depicts the convergence curves for the same parameters as in Fig. 4. Even when the convergence rate is again considerably dependent on the shape of the profile, in comparison with conductor of type **a** (see

Fig. 4) is substantially higher. The reason is that the perimeter of conductor **b** is created by longer direct parts, which is much more favorable from the viewpoint of the mesh triangulation.

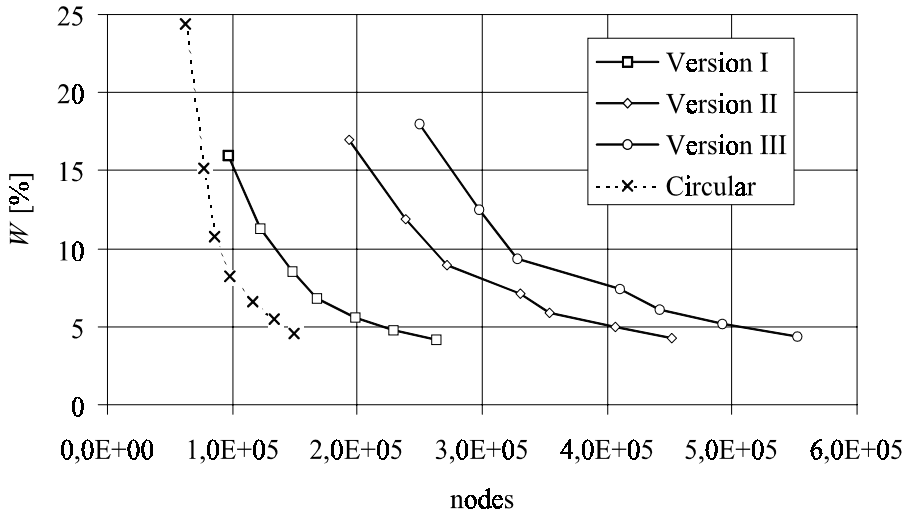

*Fig. 4. Geometrical convergence of results for the conductor of type **a** for frequency* $f = 500$ *kHz*

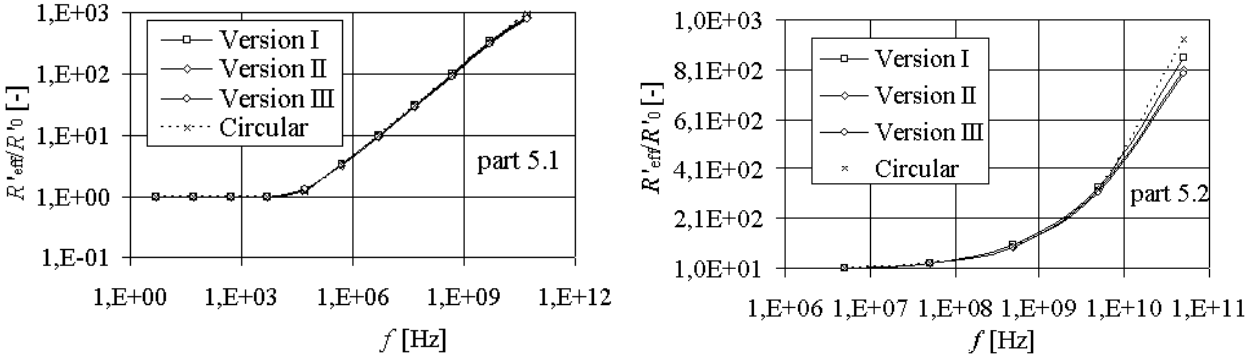

Fig. 5. Ratio of R'_{eff} / R'_0 *versus frequency for the conductor of type **a** (part 5.1) and its zoom for higher frequencies (part 5.2)*

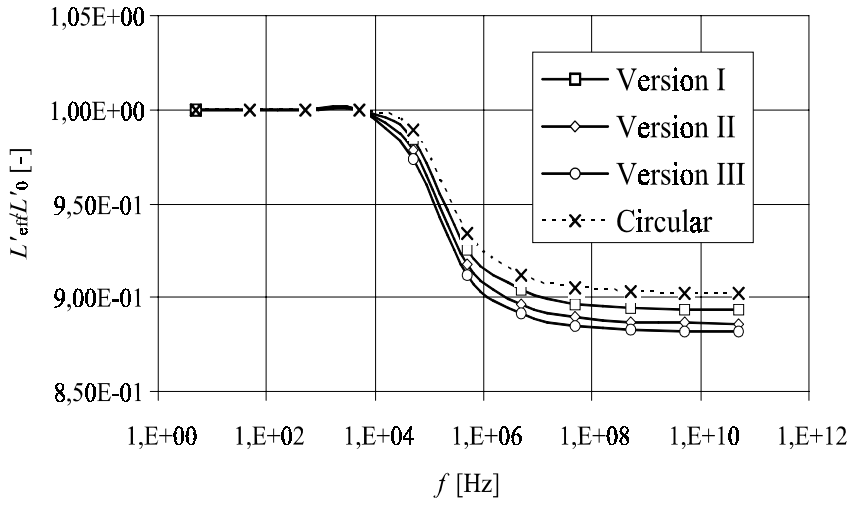

Fig. 6. Ratio of L'_{eff} / L'_0 *versus frequency for the conductor of type **a***

Fig. 6 shows the frequency-dependenct ratio of the total inductance L'_{eff} per unit length of the conductor of type **a** and circular conductor of the same cross-section related to direct-current inductance L'_0. At the first sight, some attributes of these dependencies are similar as in case of the resistance. But now the energy of magnetic field is calculated both within the conductor and air (compare equations (9) and (10)). And from certain frequencies the energy accumulated in the conductor becomes negligible with respect to the energy in the air. That is why in the interval $\langle 10^4 - 10^6 \rangle$ Hz the magnetic energy in the conductors decreases, practically to zero, which is clearly observable in the figure.

Conductor of type **b**

Fig. 8.1 depicts the frequency-dependent ratio of the effective resistance R'_{eff} per unit length of the conductor of type **b** for all two versions and direct-current resistance R'_0 of the circular conductor of the same cross-section. As the particular curves are almost identical, Fig. 8.2 contains their zoomed part, again for frequencies exceeding 1 MHz. Despite strongly expressed dependence, however, its growth is now substantially slower than in the case of conductor of type **a** (see Fig. 5.1 and 5.2). While for frequency $f = 5 \cdot 10^{10}$ Hz the ratio R'_{eff} / R'_0 for the conductor of circular profile is $9 \cdot 10^2$, for the conductor of type **a** (version II) the same ratio is $8.1 \cdot 10^2$ while for the conductor of type **b** (version II) $3.8 \cdot 10^2$. This effect is again given by the fact that the current is transferred only in very thin surface layer whose area depends practically only on its perimeter. And its value is in the case of conductor **b** much higher.

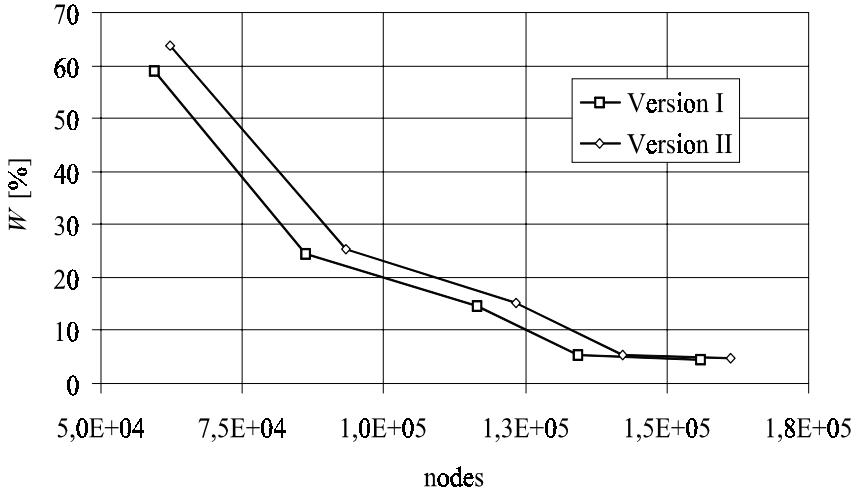

Fig. 7. Geometrical convergence of results for the conductor of type ***b*** *for frequency* $f = 500$ *kHz*

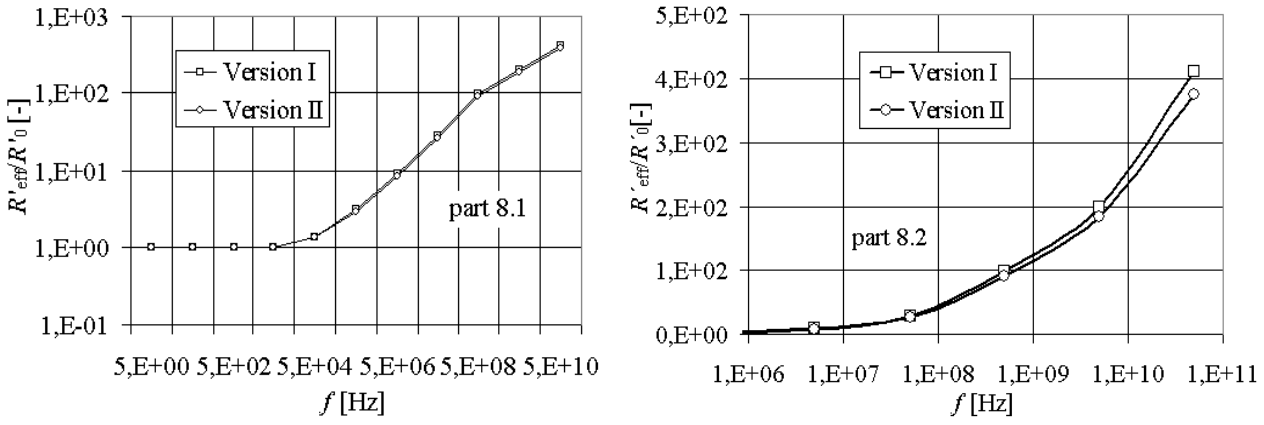

Fig. 8. Ratio of R'_{eff} / R'_0 *versus frequency for the conductor of type* ***b*** *(part 8.1) and its zoom for higher frequencies (part 8.2)*

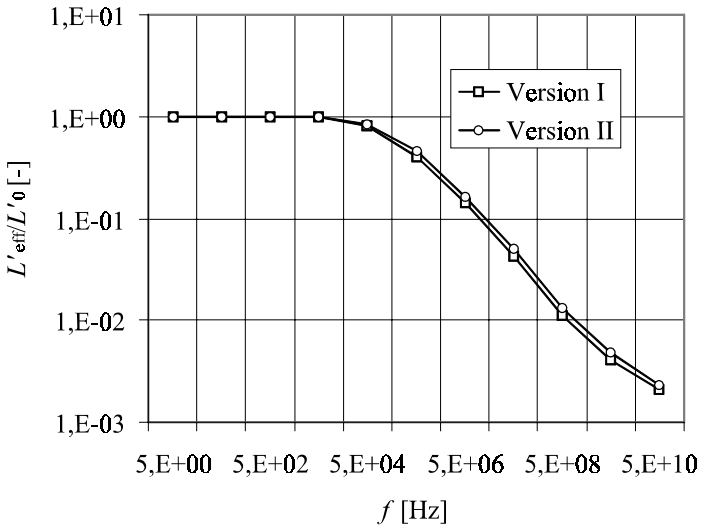

*Fig. 9. Ratio of L'_{eff} / L'_0 versus frequency for the conductor of type **b***

Fig. 9 shows the frequency dependence of the total inductance analogously as in Fig. 6. The situation is similar to that in Fig. 6, but with growing frequency the ratio L'_{eff} / L'_0 decreases much faster.

Conductor of type **c**

Convergence of solution for the conductor of type **c** follows from Fig. 10. Even in this case the necessary number of nodes exceeds 100000.

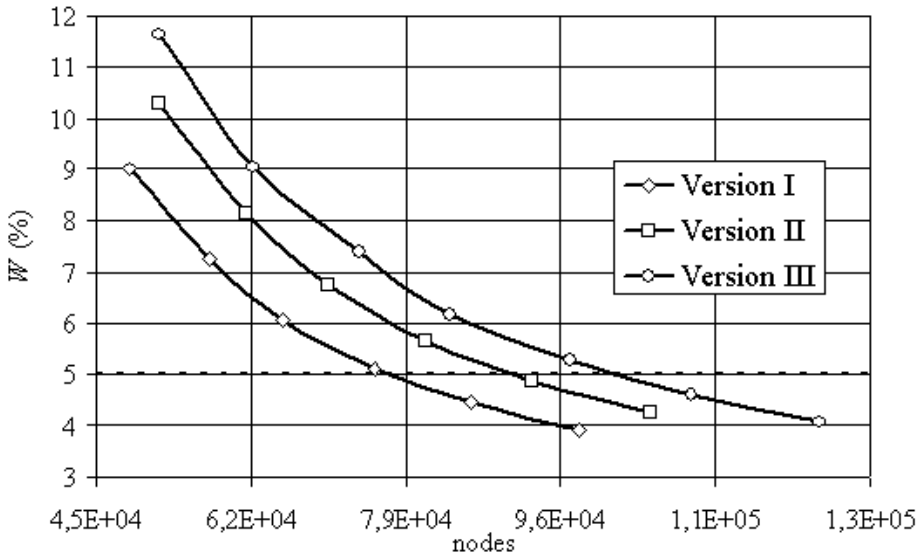

*Fig. 10. Geometrical convergence of results for the conductor of type **c** for frequency $f = 500$ kHz*

Fig. 11 contains the frequency-dependent ratio of the effective resistance R'_{eff} per unit length of the conductor of type **c** for all three versions and direct-current resistance R'_0 of the circular conductor of the same cross-section. Here the differences between the parameters of the circular conductor and band-type conductors are relatively high, as could be expected in advance. Fig. 12 finally shows the frequency dependence of the total inductance for conductor of type **c**.

The knowledge following from Figs. 10–12 is in accordance with results obtained for conductors of type **a** and **b**. On the other hand, due to long perimeter the resistances are much lower in this case. For example, the value of R'_{eff} / R'_0 for frequency $f = 5 \cdot 10^{10}$ Hz is equal $1.4 \cdot 10^2$, which is more than two times lower than for conductors of type **b**.

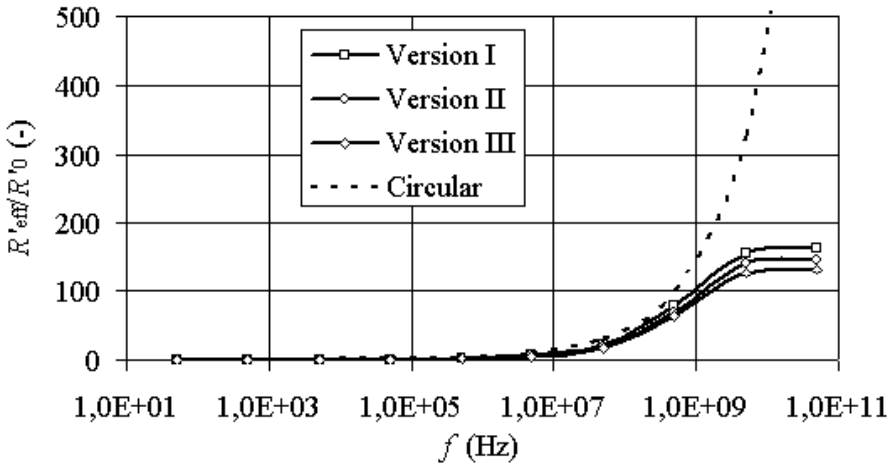

Fig. 11. Ratio of R'_{eff} / R'_0 versus frequency for the conductor of type c

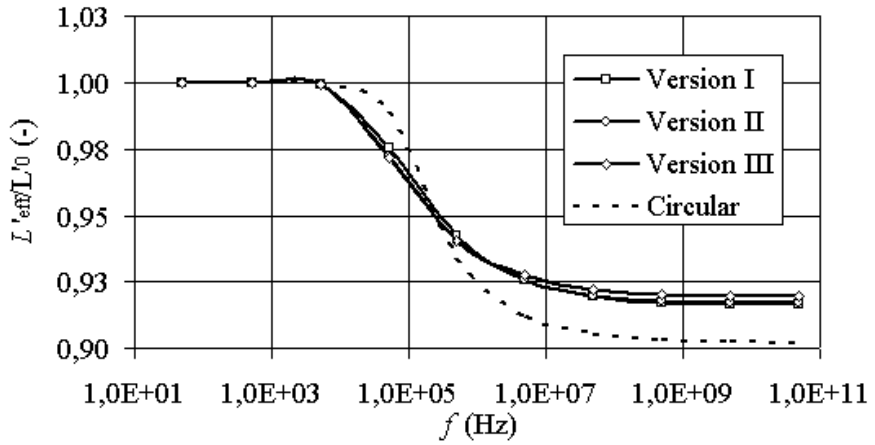

Fig. 12. Ratio of L'_{eff} / L'_0 versus frequency for the conductor of type c

Conclusion

Numerical computation of the task by differential technique requires a relatively long time because of necessity to generate a mesh with an adequate density, consisting of more than 100000 elements (the conductor itself about 20000 elements, ambient air about 80000 elements). Otherwise, it would not be possible to guarantee the convergence of results.

For frequencies up to about 1 MHz, the values of the circuit parameters of the profile conductors are comparable with the same parameters of the reference conductor with circular cross-section. For higher frequencies, however, these parameters decrease, which is particularly caused by smaller values of the resistance.

It can generally be said that the results obtained provide a hint how to choose a profile of the conductor that can satisfy requirements concerning its circuit parameters at high frequencies. Of course, design of a conductor of such a profile has to be in accordance with technological possibilities and must also satisfy viewpoints of both production and exploitation in the corresponding electronical device.

Although the differential approach is reliable and widely used for computations of this kind, sometimes it may suffer from a serious drawback consisting in considering the air domain Ω_a. Its incorporation into the definition area leads to a steep growth of elements in the discretization mesh, particularly in case of irregular cross-section of the conductor (with no condition of symmetry). Moreover, the situation deteriorates with the growing frequency, which requires very fine discretization of the conductor itself, especially in its surface layers.

That is why we started with application of integral methods for direct determination of distribution of phasor $\underline{J}_z$ of current density over the area of the profile that is given by solution of the second-kind Fredholm integral equation [3]. The circuit parameters are then calculated in accordance with formulas (6) – (11). Computations are fully realized by own program written in Borland Delphi. Of course, despite a mesh with much less elements (in comparison with meshes used in the differential approach) the computations also take a lot of time (of the order of minutes) because of necessity to work with dense matrices. Promising seems to be here application of higher-order integral methods based on the variational approach with using the Galerkin schemes, that is now being developed.

Acknowledgment

This work has been financially supported from Czech Research Plans VZ MSM 232200008 and VZ MSM 212300016.

1. Chari M.V.K, Salon S.J. Numerical methods in electromagnetism, Academic Press, San Diego, 2000. 2. www.quickfield.com (February 2003). 3. Doležel I., Karban P., Mach M., Ulrych B. Integral model of skin effect and associated phenomena in long massive conductors, Proc. PPE, Kiev, June 2004, accepted.